Supplementary Material for

Closed-Loop Control of Epilepsy by Transcranial Electrical Stimulation

Antal Berényi, Mariano Belluscio, Dun Mao, György Buzsáki*

*To whom correspondence should be addressed. E-mail: gyorgy.buzsaki@nyumc.org

Published 10 August 2012, *Science* **337**, 735 (2012)
DOI: 10.1126/science.1223154

This PDF file includes:

Closed-loop Control of Epilepsy by Transcranial Electrical Stimulation

Antal Berényi[1, 2, 3], Mariano Belluscio[1], Dun Mao[1] and György Buzsáki[1, 2*]

Supporting Material:

Materials and Methods

Surgery, electrophysiological recordings and stimulation

All experiments were approved by the institutional Animal Care and Use Committee of New York University Medical Center. Nine male Long-Evans rats (510–840 g) were implanted with intracortical recording and transcranial stimulating electrodes under isoflurane anesthesia, as described earlier (*18*). Tripolar electrodes were prepared for recording of neocortical local field potentials (LFP) and multiunit activity. Three 50-μm diameter polyimide-insulated tungsten wires (Tungsten 99.95%) were inserted into a 190-μm inner diameter stainless steel tube, and their tips were spaced 400 μm vertically from each other (Fig. 1A). The shortest wire protruded at least 4 mm from the guide tube. Impedances of the wire electrodes varied between 150-400 kΩ at 1 kHz. Ten such tripolar electrodes (30 recording channels) were implanted in each animal over the frontal and parietal cortical areas of both hemispheres. The electrodes were vertically advanced through individual holes in the skull, until the most superficial wire of the electrode reached the surface of the cortex. The hole around the electrodes was filled in with paraffin-wax, and the electrodes were fixed with dental cement.

Transcranial stimulation electrodes were constructed from the conductive end of a polyimide flexible cable. The individual interconnects of the cable were soldered together so that the current could flow equally on each of the conductive pads of the cable. The muscles were retracted from the temporal bone bilaterally. The skull was thinned using a dental drill to create a

shallow cavity for the stimulation electrodes at approximately above the barrel cortex and at the anterior midline area (2-5 mm anterior to bregma, Fig. 1B; Fig. S1) of the skull. The stimulation electrodes were placed in the cavities, with the conductive pads facing the skull, and fixed with cyano-acrylic glue to the bone, so that the conductive pads of the flex cable were completely isolated from the surrounding temporal muscles. Two miniature stainless steel screws driven into the skull above the cerebellum, served as ground and reference electrodes, respectively. A copper mesh shielding was created around the head implant to protect and electrically isolate the recording electrodes and preamplifiers from electrical noise of the environment (*29*). The connecting wires of the stimulating electrodes were brought outside the grounded copper mesh to reduce the electromagnetic interference between the stimulation and recording circuits.

The recorded signals were preamplified (20x gain) and split for recording LFP and unit activity from all sites on the one hand and for computing current source density (CSD) in real time for each tripolar electrode on the other. CSD signal was computed on-line by a custom-designed circuit, following the following formula: CSD = 2B-(A+C), where A, B, and C the electrodes positioned at equally increasing depths in the neocortex (Fig. 1). The computed CSD and the original LFP signals were further amplified 50 times, bandpass-filtered between 0.1 and 5 kHz and stored after digitization at 20 kHz sampling rate per channel. The CSD signals were virtually free of stimulation artifacts and did not saturate the amplifier even during relatively intense stimulation. Extracellular spike waveforms and local LFP components were not distorted during TES (*18*).

Nine rats with spontaneously recurring spike-and-wave (SW) episodes (*30*) were included in the present study. SW patterns were detected real time from a tripolar recording site with the best CSD signal amplitude/stimulation artifact ratio. The derived CSD trace was filtered using 4th

order analog Butterworth band-pass filter between 10 and 130 Hz. The spike components of the SW patterns were detected as voltage crossings at a preset threshold level using an analog voltage comparator after inverting and half-wave rectifying the CSD signal. The generated 'spike detection signal' was used to trigger TES. To avoid false detection of spurious spikes due to the stimulation artifacts, the stimulator was gated using a re-triggerable monostable multivibrator with a 80 msec protective delay. In addition, the threshold signal was integrated so that a pulse was generated only if at least 2 CSD spikes occurred within 200 ms. This procedure prevented TES pulses to be triggered by cable movement-generated and other transient artifacts.

Closed-loop transcranial electrical stimulation

Transcranial alternating current stimulation was performed with two electrode configurations (*18*). For equal intensity and polarity stimulation of both hemispheres, the frontal midline electrode was chosen as one polarity and the two connected parietal electrodes as the opposing polarity. Alternatively, the stimulation was delivered to the left and right parietal electrodes. Both stimulus combinations were tested in each animal, and the configuration with the highest modulation index (see below) was selected for testing the effect of TES on SW activity. Stimulation signals were generated by a computer-controlled waveform generator, and capacitance-isolated by a precision isolation amplifier circuit. The floating (animal) side of the circuit was powered using two 9 V batteries. Two different stimulus waveforms were used in all experiments. A continuous 1-Hz sinusoid stimulus of various intensities was used to examine neuronal entrainment in the initial experiments. For the closed-loop TES experiments, a 50-ms long Gaussian waveform, triggered by the SW detection signal, was employed. The delay

between the spike component of the SW and the stimulus onset was 0, 10 or 40 ms so that TES coincided with the spike, the onset or the peak of the wave component of the SW pattern.

The strength of the intracerebral voltage gradient was calculated as a mean ratio of amplitude differences across pairs of recording electrodes in the axis of the stimulation and their spatial distances. The maximum stimulus amplitudes used in this study (4-5 V peak-to-peak) generated approximately 10 mV/mm voltage gradients, while the threshold for TES entrainment of neurons was approximately 1 mV/mm (*18*). For sham stimulation, the animal was disconnected from the stimulus isolation unit. Each TES session consisted of multiple (n = 5 to 24) 10-min sham and 10-min TES epochs while the rat was sitting still in the home cage. TES sessions were repeated daily to examine the consistency of the TES effect across days and to test the effect of different intensities. The 'spike detection signal', the gating signals, and the pre-isolation stimulus signal were also recorded and stored.

Movement detection

To detect SW or TES-related movements, a 3-dimensional accelerometer was incorporated into the head stage (bandwidth: 500 Hz; ± 30 m/s^2 maximum sensitivity). The SW- or TES-triggered movement vector was calculated from the acceleration signals along the 3 main axes. High intensity of stimulation occasionally induced visible and detectable twitches or head movements (Fig. S4). SW patterns were also associated with detectable head movements in a few rats (*30*). The mean head movement acceleration was calculated separately for SW episodes and for interictal (control) periods for both sham and TES recording sessions. These tests served to select TES intensities, which were subthreshold to induce significantly larger head movements than present during sham stimulation. In several animals, we also examined the effect of TES on the

brain state. In agreement with a previous observation (*18*), TES did not induce arousal during sleep. To examine the potential arousal effect of TES, time resolved LFP spectra were analyzed during wake-sleep transitions and sleep. The LFP signal was transformed into the time-frequency domain using a multitaper Fourier transformation, and after whitening of the spectrogram, the brain state (awake vs sleep; REM vs. non-REM) was quantified on the basis of the theta/delta (4-8 Hz versus 1-4 Hz) and beta/delta (16-20 Hz vs 1-4 Hz) power ratio in 1-sec long windows (Fig. S3). These control tests were carried out to exclude the possibility that TES induced modification of SW activity was brought about by a secondary effect of sensory feedback or a generalized state change of the brain (*18*).

Data analysis

Detection of individual SW episodes was performed offline using a semi-automated method. SW episodes were detected from the off-line derived CSD signals. Similar to the on-line detection, the LFP was band-pass filtered with a 4^{th} order zero phase lag Butterworth filter between 10 and 130 Hz, and the peaks of the spike components, exceeding 2 standard deviation (SD) of the baseline activity, were detected. SW episodes were separately detected from each brain recording sites. For the determination of the duration of SW episodes, the detected durations were averaged. The threshold of spike detection was manually re-adjusted in cases when the automatic detection generated false positive or false negative events. Consecutive SW episodes were considered separate (i.e., non-continuous) if at least a 1-sec gap was present between them. Events containing less than 3 spike components were excluded from the analysis. Multiple unit activity (MUA) was detected from the high-pass filtered (600 Hz) signals. Multiple unit spikes were generated by automated clustering and manual cluster cutting (*31*).

Instantaneous stimulus phase information for SW events and multiunit activity was calculated by Hilbert-transformation of the recorded 1-Hz stimulus waveform. TES-modulation of unit firing was computed for both control epochs and SW episodes. MUA phase histograms were statistically evaluated by Rayleigh-test for circular data against a randomized uniform circular distribution of the same dataset (phase tags were randomized in the range of $\pm\pi$ radians). To determine the effect of TES on unit firing probability and the amplitude of SW activity, the data was binned into 10 bins of equal sizes (36^o each). Within each bin, 100-ms long LFP segments and multiple unit firing were realigned to the peak of the spike component of SW episodes (-20 before to +80 ms after the peak). A mean LFP waveform was calculated within each bin after linearly de-trending the individual LFP segments from multiple SW episodes. The amplitude of the spike component of SW was determined as a voltage difference between the peak of the LFP spike and the baseline (Fig. 2). TES phase-dependent modulation index (MI) was calculated for the binned LFP patterns as the ratio of the difference and sum of the smallest and largest mean spike amplitudes. Modulation index for the multiple unit firing patterns were calculated in a similar way but using the firing rates during the spike components of SW (± 10 ms surrounding the LFP spike). Effectiveness of TES on LFP and MUA activity was tested statistically by performing a Student's t-test on paired samples on the binned modulation indices against randomly shuffled phase data.

TES sinusoid trains at 1 Hz (10 min) were applied during both control and spontaneously occurring SW patterns. Preliminary experiments established that the threshold of voltage gradient for entraining neurons was 1mV/mm (generated by approximately ±0.5V stimulation amplitude at 1 Hz and 0.1 mA current), whereas > ±6 V intensity induced arousal and movement ((*18*); Fig. S4). Therefore, in subsequent experiments intensities between 0.5 and ±5 V were

used, which never induced any overt behavioral effects. The maximum tolerated stimulus intesity was individually determined for each animal. The peak of the stimulus was used to construct event-related firing histograms. A modulation index was calculated by dividing the difference of maximum and minimum values during the opposite polarities of the stimulus by the sum of maximum and minimum values.

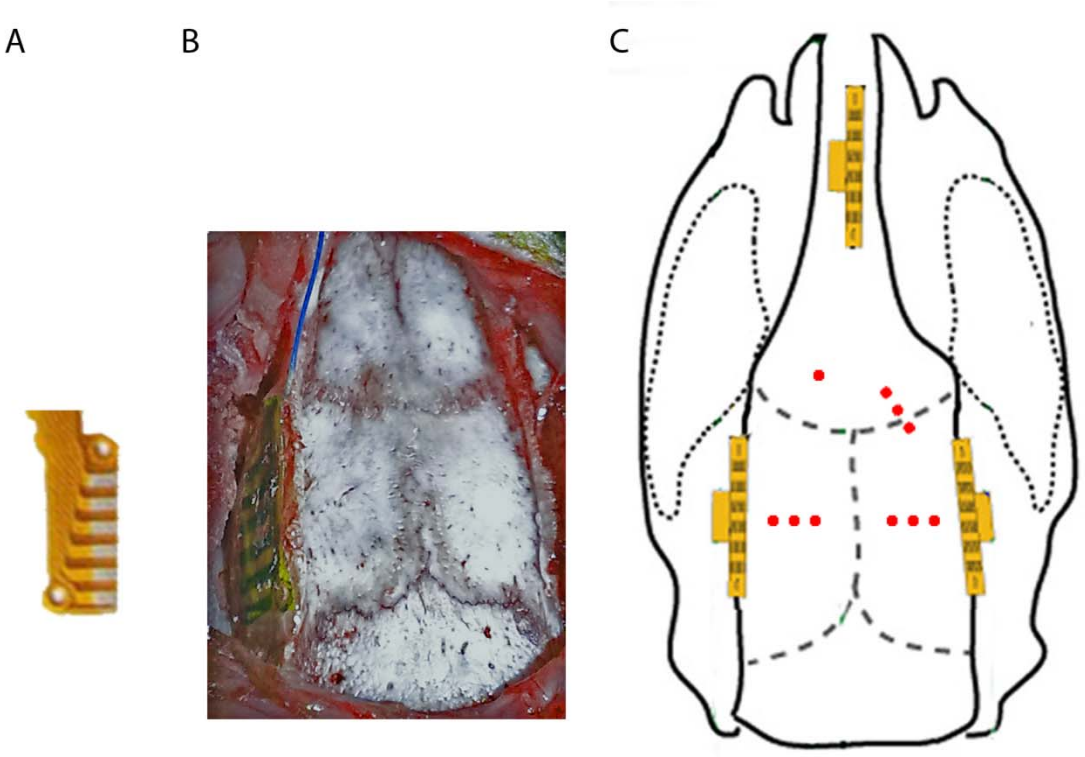

Fig S1. TES electrodes. A. The conductor end of the polyimide flex cable used as a stimulation plate. B. Stimulation plate *in situ* placed on the left temporal bone during surgery. Conductive side of the plate is facing the skull. Non-conductive side and the edges of the cable are sealed by cyanoacrylate glue. C. Schematics of the locations of the implanted stimulating plates (yellow-grey) and intracortical tripolar wire electrodes (red dots). Each individual red dot corresponds to a tripolar electrode.

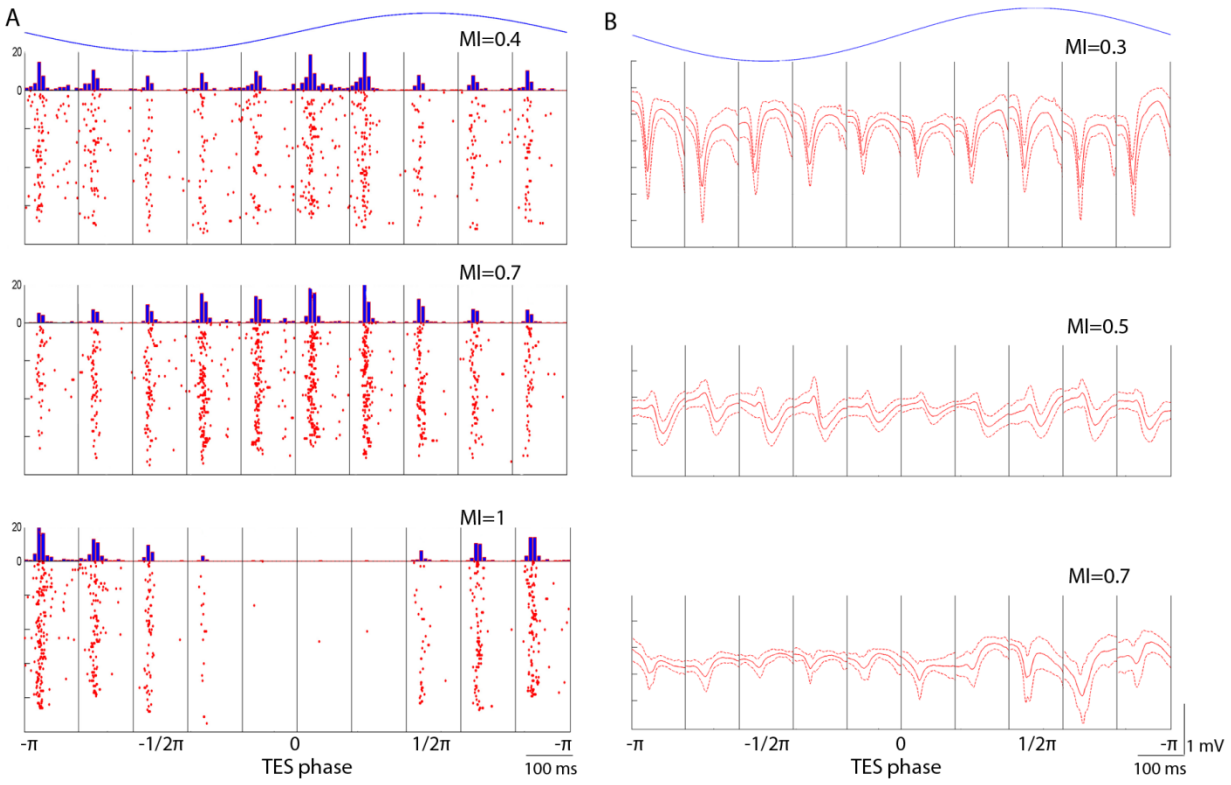

Fig. S2. Modulation of cortical excitability by 1 Hz TES stimulation. A. Stimulus waveform is denoted on top. Examples of the modulation index (MI) of spike component-related firing in 3 different rats as a function of the TES phase. B. Examples of the modulation index of the LFP spike amplitude of SW in 3 different rats.

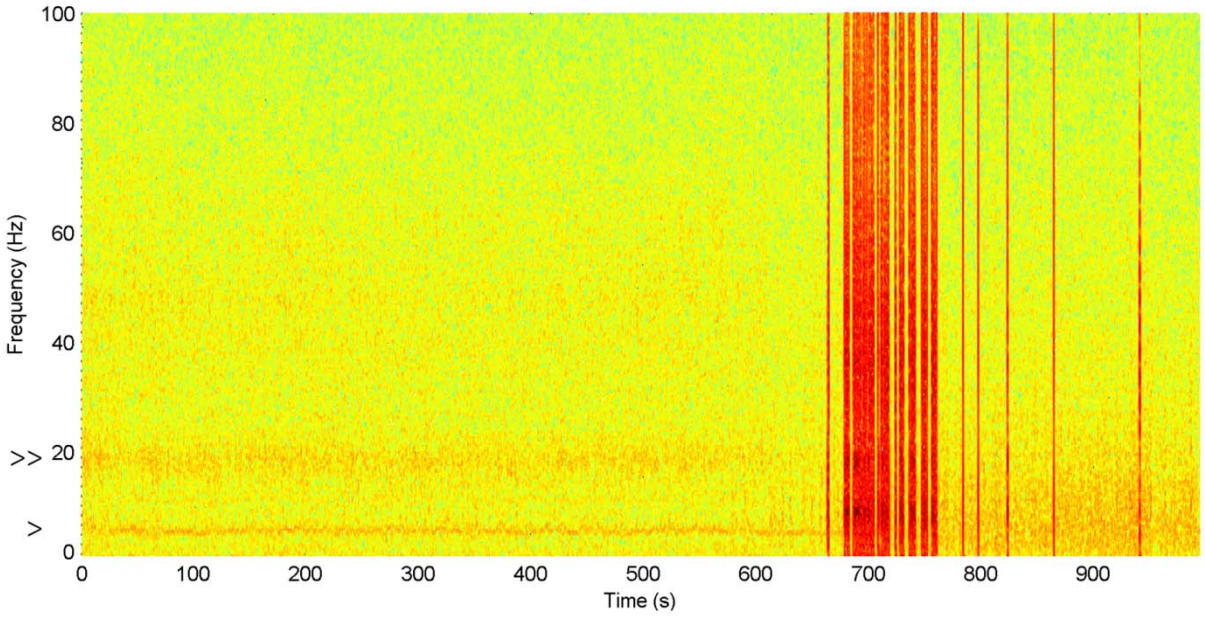

Fig. S3. Low frequency TES does not induce arousal. Time-resolved spectral power of LFP recorded from the parietal cortical area during wake-sleep transition. During the first 600 sec, the rat was exploring the home cage. Note high power in the theta (arrow), beta (double arrow, i.e., second harmonic of theta) and low gamma frequency (30-60 Hz) bands. Note also the lack of SW episodes during exploration (lack of TES artifacts). SW episodes occurred maximally during waking immobility (*30*) starting at 660 sec, as indicated by the TES artifacts (red lines). No artifact suppression was used to highlight SW-triggered TES. The rat fell asleep between 700 and 750 sec. Note the lack of changes in spectral power following TES stimulation, indicating that TES did not induce detectable arousal.

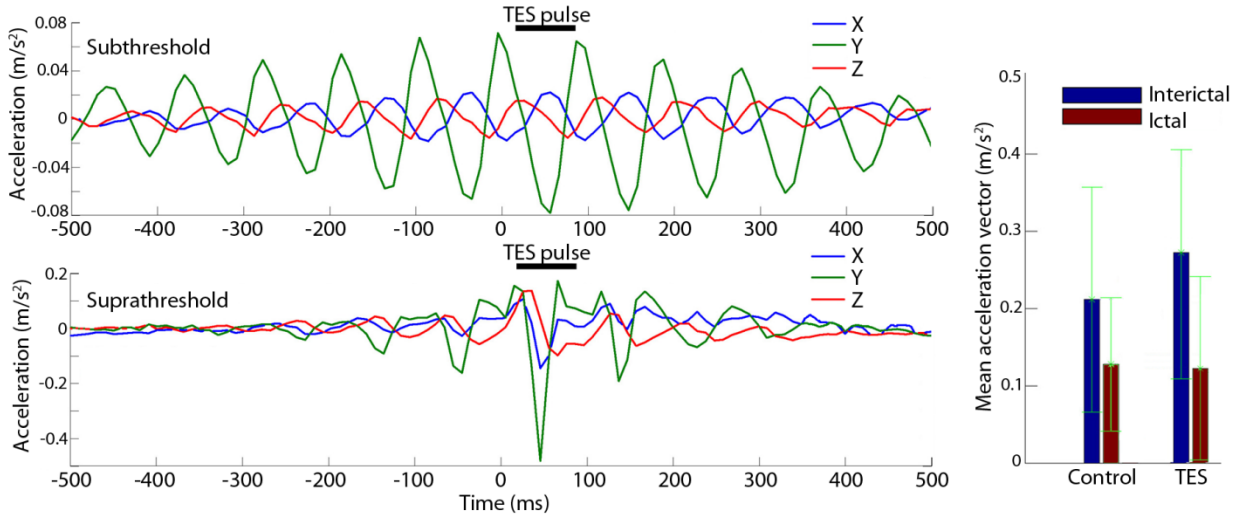

Fig. S4. SW and TES-induced head movements. Top, Averages of the accelerometer generated signals (x, y and z planes), triggered by the spike component of SW episodes. In this example rat, SWs were often associated with visible whisker and head movements (*30*). Bottom, Averages of accelerometer generated signals, triggered by TES pulses at high intensity (±5.5V). Note TES-enhanced head movement at 40 ms. For the evaluation of TES on SW episodes only intensities subthreshold to head-movement induction (< 2 SD of no-TES baseline) were used to eliminate potential sensory feedback-induced secondary effects. Right panel: mean acceleration vector (motor activity) during interictal and ictal periods with and without TES (data are averaged across all sessions in all animals). Note that there is no significant difference in ictal motor activity between stimulated and control sessions.

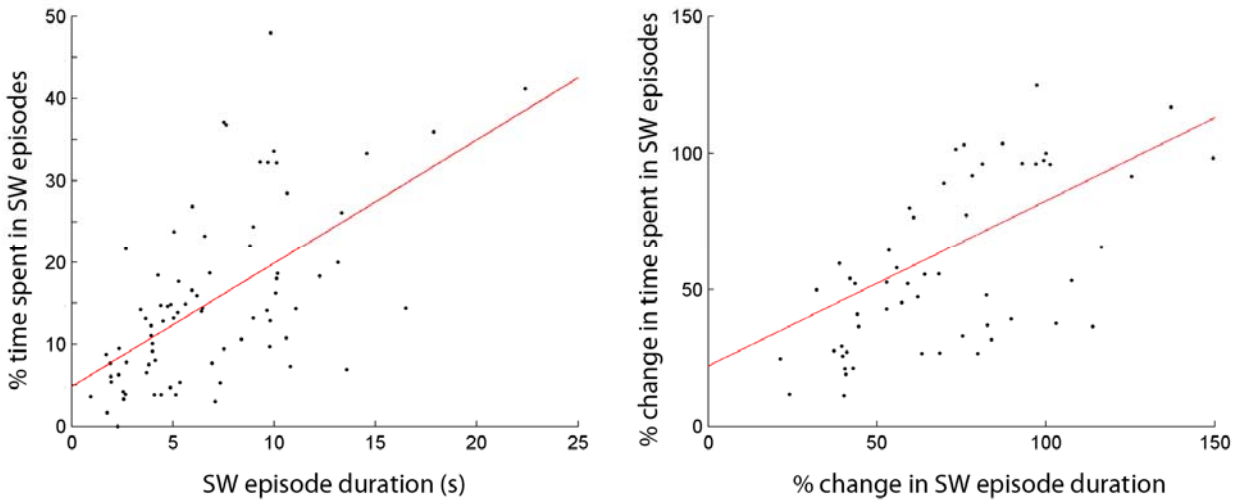

Fig. S5. Correlations between the mean duration and percent time spent in SW episodes in a given session. Left panel: Correlation between the duration of SW episodes and percent of time spent in SW periods. Each dot represents mean values in a given session. Right panel: Correlation between the TES-induced reduction of SW duration and the reduction of time spent in SW.

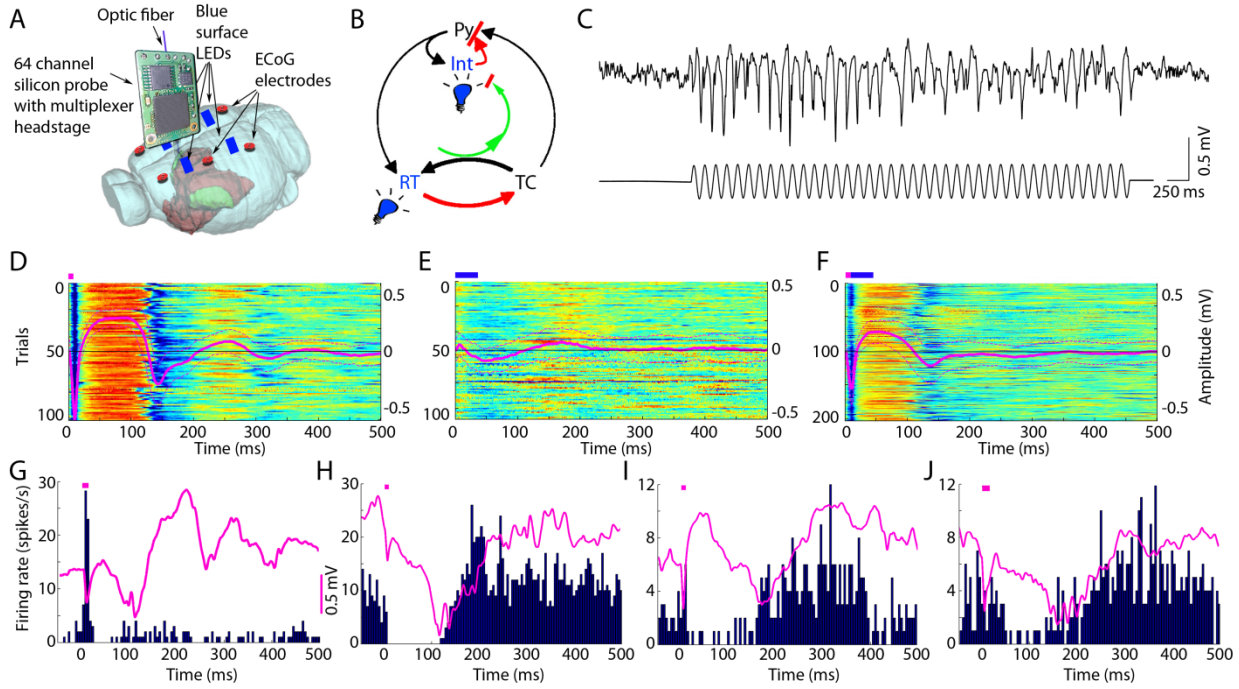

Fig. S6. Breaking the excitatory reverberation in the thalamocortical loop by optogenetic suppressing of cortical circuits. A. Experimental setup. An etched optic fiber was placed onto an 8-shank silicon probe (*32*) and implanted into the reticular nucleus of thalamus to induce SW pattern (*33*, *34*). Blue LEDs (squares) were placed epidurally at two positions on each side. Cortical surface LFP activity (ECoG) was monitored by epidural screw electrodes. Pvalb-IRES-Cre;Ai32 double transgenic mice (n = 4), expressing ChR2 in parvalbumin type interneurons were used (*34*). B. Reverberation in the thalamocortical loop. Interactions between the reticular nucleus (RT) and thalamocortical (TC) neurons form the basis of the thalamic rhythm (black, excitatory; red, inhibitory connections; (*35*)). The cortico-thalamic loop amplifies these oscillations (*36*). Blue light stimulation of the RT neurons induces corticothalamic oscillations, whereas light stimulation of cortical PV interneurons (Int) induces rebound excitation in cortical pyramidal cells (Py). Feedback excitation during the wave (silent) period of SW activity is hypothesized to interfere with thalamo-cortical amplification. C. Induced SW activity by repetitive stimulation of RT parvalbumin-expressing (ChR2) neurons. D-F. On alternate trials, a

single light pulse was delivered to the reticular nucleus (RT – laser; 5 msec; magenta line on top of panel D), to the neocortex via LEDs (E; 30 msec; blue line) or both (F). Each line corresponds to a single trial, where color coding corresponds to amplitude. Red and blue colors correspond to positive (neuronal 'silence') and negative polarity components, respectively. Note single pulse induction of SW activity (left panel) and suppression of SW by closed-loop light activation of the neocortex (right panel). Averaged traces (mean and SD) are superimposed on the panels. G. Light-induced discharge of RT neurons and LFP. H. Thalamocortical neuron. Note strong delayed suppression and rebound spiking activity. I-J. Two neocortical neurons. Note delayed suppression and rebound spiking activity. Suppression of neuronal firing corresponds to the wave component of SW. C-F, waking mouse, G-J urethane anesthesia.

References and Notes

1. C. Hammond, H. Bergman, P. Brown, Pathological synchronization in Parkinson's disease: Networks, models and treatments. *Trends Neurosci.* **30**, 357 (2007). doi:10.1016/j.tins.2007.05.004 Medline

2. H. S. Mayberg *et al*., Deep brain stimulation for treatment-resistant depression. *Neuron* **45**, 651 (2005). doi:10.1016/j.neuron.2005.02.014 Medline

3. J. S. Perlmutter, J. W. Mink, Deep brain stimulation. *Annu. Rev. Neurosci.* **29**, 229 (2006). doi:10.1146/annurev.neuro.29.051605.112824 Medline

4. O. Makeyev, X. Liu, K. Koka, S. M. Kay, W. G. Besio, Transcranial focal stimulation via concentric ring electrodes reduced power of pentylenetetrazole-induced seizure activity in rat electroencephalogram. *Conf. Proc. IEEE Eng. Med. Biol. Soc.* **2011**, 7560 (2011). Medline

5. G. K. Motamedi *et al*., Optimizing parameters for terminating cortical afterdischarges with pulse stimulation. *Epilepsia* **43**, 836 (2002). doi:10.1046/j.1528-1157.2002.24901.x Medline

6. S. J. Schiff *et al*., Controlling chaos in the brain. *Nature* **370**, 615 (1994). doi:10.1038/370615a0 Medline

7. G. Girardeau, K. Benchenane, S. I. Wiener, G. Buzsáki, M. B. Zugaro, Selective suppression of hippocampal ripples impairs spatial memory. *Nat. Neurosci.* **12**, 1222 (2009). doi:10.1038/nn.2384 Medline

8. U. Najib, S. Bashir, D. Edwards, A. Rotenberg, A. Pascual-Leone, Transcranial brain stimulation: clinical applications and future directions. *Neurosurg. Clin. N. Am.* **22**, 233, ix (2011). doi:10.1016/j.nec.2011.01.002 Medline

9. B. Rosin *et al*., Closed-loop deep brain stimulation is superior in ameliorating parkinsonism. *Neuron* **72**, 370 (2011). doi:10.1016/j.neuron.2011.08.023 Medline

10. E. T. Varga *et al*., Transcranial direct current stimulation in refractory continuous spikes and waves during slow sleep: A controlled study. *Epilepsy Res.* **97**, 142 (2011). doi:10.1016/j.eplepsyres.2011.07.016 Medline

11. M. J. Morrell; RNS System in Epilepsy Study Group, Responsive cortical stimulation for the treatment of medically intractable partial epilepsy. *Neurology* **77**, 1295 (2011). doi:10.1212/WNL.0b013e3182302056 Medline

12. R. Fisher *et al*.; SANTE Study Group, Electrical stimulation of the anterior nucleus of thalamus for treatment of refractory epilepsy. *Epilepsia* **51**, 899 (2010). doi:10.1111/j.1528-1167.2010.02536.x Medline

13. R. S. Fisher, Therapeutic devices for epilepsy. *Ann. Neurol.* **71**, 157 (2012). doi:10.1002/ana.22621 Medline

14. J. R. Hughes, Absence seizures: A review of recent reports with new concepts. *Epilepsy Behav.* **15**, 404 (2009). doi:10.1016/j.yebeh.2009.06.007 Medline

15. C. Marescaux, M. Vergnes, A. Depaulis, Genetic absence epilepsy in rats from Strasbourg—a review. *J. Neural Transm. Suppl.* **35**, 37 (1992). Medline

16. F. Fröhlich, D. A. McCormick, Endogenous electric fields may guide neocortical network activity. *Neuron* **67**, 129 (2010). doi:10.1016/j.neuron.2010.06.005 Medline

17. M. A. Nitsche, W. Paulus, Noninvasive brain stimulation protocols in the treatment of epilepsy: Current state and perspectives. *Neurotherapeutics* **6**, 244 (2009). doi:10.1016/j.nurt.2009.01.003 Medline

18. S. Ozen *et al*., Transcranial electric stimulation entrains cortical neuronal populations in rats. *J. Neurosci.* **30**, 11476 (2010). doi:10.1523/JNEUROSCI.5252-09.2010 Medline

19. R. A. Joundi, N. Jenkinson, J. S. Brittain, T. Z. Aziz, P. Brown, Driving oscillatory activity in the human cortex enhances motor performance. *Curr. Biol.* **22**, 403 (2012). doi:10.1016/j.cub.2012.01.024 Medline

20. L. Marshall, H. Helgadóttir, M. Mölle, J. Born, Boosting slow oscillations during sleep potentiates memory. *Nature* **444**, 610 (2006). doi:10.1038/nature05278 Medline

21. Materials and methods are available as supplementary materials on *Science* Online.

22. A. Kandel, G. Buzsáki, Cellular-synaptic generation of sleep spindles, spike-and-wave discharges, and evoked thalamocortical responses in the neocortex of the rat. *J. Neurosci.* **17**, 6783 (1997). Medline

23. G. Kostopoulos, P. Gloor, A. Pellegrini, J. Gotman, A study of the transition from spindles to spike and wave discharge in feline generalized penicillin epilepsy: Microphysiological features. *Exp. Neurol.* **73**, 55 (1981). doi:10.1016/0014-4886(81)90045-5 Medline

24. M. Steriade, Sleep, epilepsy and thalamic reticular inhibitory neurons. *Trends Neurosci.* **28**, 317 (2005). doi:10.1016/j.tins.2005.03.007 Medline

25. J. Engel, Jr. *et al*., Practice parameter: temporal lobe and localized neocortical resections for epilepsy. *Epilepsia* **44**, 741 (2003). doi:10.1046/j.1528-1157.2003.48202.x Medline

26. A. Jackson, E. E. Fetz, Interfacing with the computational brain. *IEEE Trans. Neural Syst. Rehabil. Eng.* **19**, 534 (2011). doi:10.1109/TNSRE.2011.2158586 Medline

27. N. G. Hatsopoulos, J. P. Donoghue, The science of neural interface systems. *Annu. Rev. Neurosci.* **32**, 249 (2009). doi:10.1146/annurev.neuro.051508.135241 Medline

28. A. Rotenberg, A. Pascual-Leone, Safety of 1 Hz repetitive transcranial magnetic stimulation (rTMS) in patients with titanium skull plates. *Clin. Neurophysiol.* **120**, 1417 (2009). doi:10.1016/j.clinph.2009.05.004 Medline

29. M. Vandecasteele *et al*., Large-scale recording of neurons by movable silicon probes in behaving rodents. *J. Vis. Exp.* **61**, e3568 (2012). Medline

30. G. Jandó *et al*., Spike-and-wave epilepsy in rats: Sex differences and inheritance of physiological traits. *Neuroscience* **64**, 301 (1995). doi:10.1016/0306-4522(94)00329-4 Medline

31. K. D. Harris, D. A. Henze, J. Csicsvari, H. Hirase, G. Buzsáki, Accuracy of tetrode spike separation as determined by simultaneous intracellular and extracellular measurements. *J. Neurophysiol.* **84**, 401 (2000). Medline

32. S. Royer *et al*., Control of timing, rate and bursts of hippocampal place cells by dendritic and somatic inhibition. *Nat. Neurosci.* **15**, 769 (2012). doi:10.1038/nn.3077 Medline

33. M. M. Halassa *et al*., Selective optical drive of thalamic reticular nucleus generates thalamic bursts and cortical spindles. *Nat. Neurosci.* **14**, 1118 (2011). doi:10.1038/nn.2880 Medline

34. L. Madisen *et al*., A toolbox of Cre-dependent optogenetic transgenic mice for light-induced activation and silencing. *Nat. Neurosci.* **15**, 793 (2012). doi:10.1038/nn.3078 Medline

35. M. Steriade, D. A. McCormick, T. J. Sejnowski, Thalamocortical oscillations in the sleeping and aroused brain. *Science* **262**, 679 (1993). doi:10.1126/science.8235588 Medline

36. N. Leresche, R. C. Lambert, A. C. Errington, V. Crunelli, From sleep spindles of natural sleep to spike and wave discharges of typical absence seizures: Is the hypothesis still valid? *Pflugers Arch.* **463**, 201 (2012). doi:10.1007/s00424-011-1009-3 Medline